Preparation of amorphous Fe_2O_3 powder with different particle sizes

X. Cao,[a] Yu. Koltypin,[a] R. Prozorov,[b] G. Kataby[a] and A. Gedanken*[a]

[a]*Department of Chemistry, Bar-Ilan University, Ramat-Gan 52900, Israel*

[b]*Department of Physics, Bar-Ilan University, Ramat-Gan 52900, Israel*

A method for the preparation of amorphous Fe_2O_3 powder with particle size of about 25 nm is reported. The amorphicity of Fe_2O_3 nanoparticles was determined by X-ray diffraction (XRD), and by electron diffraction measurements. The control of the particle size has been demonstrated by transmission electron microscopy (TEM), differential scanning calorimetry (DSC), thermogravimetry (TG), surface area measurements (BET) and Quantum Design SQUID magnetization measurements. The magnetization of pure amorphous Fe_2O_3 is very low (<5 emu g^{-1}) and it crystallizes at 285 ± 10 °C. The measured properties demonstrated a strong dependence of the particle size on the concentration of $Fe(CO)_5$ in decalin. The more dilute the solution, the smaller the particle size of the amorphous Fe_2O_3 product obtained.

Amorphous metal oxides have many important applications including solar energy transformation, magnetic storage media, use in the electronics industry and also as catalysts.[1–5] Much research has been carried out in the last 20 years on the manufacture of amorphous oxides and their characteristics. Almost all of the amorphous transition metal oxides that have been conventionally produced exhibit superparamagnetic or paramagnetic behavior.[6] Amorphous metal oxides can be obtained by rapidly quenching a molten mixture of metal oxides and a glass former such as P_2O_5, V_2O_5, Bi_2O_3, SiO_2, CaO, *etc.*[1,6,7,8] or by thermal decomposition of some easily decomposed metal compounds.[4,9] Amorphous metal oxide thin films on a substrate can be prepared by means of ion beam sputtering, electron beam evaporation or thermal evaporation.[10] So far, only a few pure amorphous metal oxides such as Cr_2O_3, V_2O_5, MnO_2 and PbO_2 powders have been successfully prepared by means of thermal decomposition.[4,9] Other amorphous metal oxides are usually obtained in the form of hydrous oxides.[5,11] Cooling rates of *ca.* 10^5–10^7 K s^{-1} are generally required to prepare amorphous metals.[12] The thermal conductivities of metal oxides are usually much lower than those of metals. Therefore, it seems to be more difficult to prepare amorphous metal oxides than amorphous metals, since larger cooling rates are required for their preparation. This is the reason why amorphous metal oxides can only be obtained in the form of thin films and why a glass former must be used to prevent crystallization of metal oxides if the quenching method is applied.

Suslick *et al.* have successfully prepared pure amorphous iron,[12] amorphous cobalt, amorphous Fe/Co alloy[13] and amorphous molybdenum carbide[14] by means of sonication. The heating and cooling rates during cavitational collapse are estimated to be $>2\times10^9$ K s^{-1} and may be as large as 10^{13} K s^{-1}.[12] The magnetic properties of amorphous iron nanoparticles were also studied thoroughly by Suslick and coworkers.[15] Recently, we have successfully prepared a series of amorphous iron powders with different particle sizes.[16] During the sonication of $Fe(CO)_5$ in decane under Ar, we have found that the lower the concentration of the $Fe(CO)_5$ in decane solution, the smaller is the particle size of amorphous iron. A new and convenient method for the preparation of pure amorphous Fe_2O_3 powder has been developed by us and reported elsewhere.[17] We have also prepared amorphous nanometer sized particles of nickel[18] and used this preparation method to coat silica particles with 5–10 nm size amorphous nickel particles.[19]

Here, we combine our method for the preparation of amorphous Fe_2O_3[17] with our technique of controlling the particle size of amorphous iron.[16] We demonstrate that this combination enables us to synthesize amorphous Fe_2O_3 nanoparticles the size of which can be controlled.

Experimental

The preparation of amorphous Fe_2O_3 is similar to that of amorphous Fe. Neat $Fe(CO)_5$ (Aldrich) or a solution in decalin (Fluka) of concentration 4, 1 or 0.25 M was irradiated with a high intensity ultrasonic horn (Ti-horn, 20 KHz) under 1.5 atm of air at 0 °C for 3 h. The products were washed thoroughly with dry pentane. All these preparation procedures were performed under a normal air atmosphere. To remove any solvents or starting material that might be adsorbed to the surface of the nanoparticles we usually heated the sample to 130 °C under vacuum or under argon for 3 h. Absence of the starting material was checked by FTIR measurements of the CO band at *ca.* 2000 cm^{-1}. Elemental analysis by EDX (energy dispersive X-ray analysis) established that the black powder contains Fe and O with only a small amount of C (estimated $<2\%$). An additional, and more accurate measurement to determine the concentration of the impurities was carried out using an elemental analyzer (CE Instrument EA 1110). The product of the sonication of pure $Fe(CO)_5$ was found to contain 3.54% carbon and 0.12% hydrogen. Since the main contaminant in this case is the precursor or one of its decomposition products [$Fe_3(CO)_{12}$], the analysis was repeated after heating the product at 130 °C for 3 h. The results revealed a drop in the concentration of carbon to 2.9% and the amount of hydrogen remained unchanged. Nitrogen was not observed in our samples.

XRD (X-ray diffraction) was carried out on a Model-2028 (Rigaku) diffractometer (scanning rate = 0.5 ° min^{-1}, Cu-Kα_1). Two analytical methods were used to confirm the absence of Fe^{2+} ions in our product. In the first, a spot test[20] using α,α'-phenanthroline was performed. In the second, the Fe^{3+} content was determined by an iodometric titration as described below: an accurately weighed amount (*ca.* 15 mg) of the sample was placed in a flask to which 3 g of solid KI was added. A 1:1 solution of HCl–H_2O was added to the flask (20 ml). The liberated iodine was titrated against a standard $Na_2S_2O_3$ solution with starch as an indicator. The two methods indicated that the sonication product is composed of only Fe^{3+} ions. The amorphous Fe_2O_3 product was converted to crystalline Fe_3O_4 in the following manner: 0.15 g of the amorphous powder were heated in an evacuated sealed quartz tube

(10^{-6} Torr) at 450 °C for 4 h and then quenched to room temperature. In order to reduce the oxygen concentration, the tube was flushed several times with an inert gas before sealing. This sample was identified as crystalline Fe_3O_4. This is not surprising since the literature reports[21] that heating Fe_2O_3 in vacuum to 250 °C yields Fe_3O_4. If the amorphous Fe_2O_3 is heated under oxygen at 370 °C for 3 h γ-Fe_2O_3 is obtained. A prolonged heating of the amorphous Fe_2O_3 for 24 h at 430 °C yields α-Fe_2O_3. The nature of the products was examined by Mössbauer spectroscopy[17] as well as magnetization measurements. We have coupled the TG measurements with magnetic measurements by placing the sample in a Mettler TGA 4000 equipped with a small permanent magnet. DSC studies were carried out on a Mettler DSC 30. Magnetization measurements were performed on a Quantum Design MPMS SQUID magnetometer. Particle size analysis was carried out on a COULTER Model N4. The surface area was measured using the BET (Micromeritics Gemini) nitrogen gas adsorption method.

Results and Discussion

XRD, TEM and particle size analysis

The amorphous nature of the product is demonstrated by its XRD spectrum as well as by electron diffraction patterns. A diffuse ring pattern is detected for the sonication product indicating its amorphous nature. The XRD of the product before and after heat treatment is depicted in Fig. 1 and demonstrates clearly the amorphicity of the as-prepared sonication product. Combining this information and the chemical analysis results we conclude that the sonication product is amorphous powdered Fe_2O_3. The conversion of the amorphous Fe_2O_3 into the crystalline form occurs when the sample is heated in oxygen and γ-Fe_2O_3 is obtained.[17] On the other hand, when the amorphous sample is heated in vacuum or in nitrogen (420 °C) crystalline Fe_3O_4 is obtained. The XRD of the crystalline Fe_3O_4 and a sample of commercial Fe_3O_4 powder (Aldrich, 98%) are also shown in Fig. 1. The XRD pattern of Fe_3O_4 is different from those of α,γ-Fe_2O_3 and pure Fe. The XRD pattern of Fe_3O_4 (ASTM card 19-629) and γ-Fe_2O_3 (ASTM card 24-81) are almost identical. The main difference between these two patterns is that γ-Fe_2O_3 shows three peaks ($d=3.73$ Å, $I/I_1=5\%$; $d=2.78$ Å, $I/I_1=19\%$; $d=2.32$ Å, $I/I_1=6\%$) that Fe_3O_4 does not. It can be concluded that after heating *in vacuo* or in N_2 the product is crystalline Fe_3O_4. On the other hand, if the heating is carried out under O_2, γ-Fe_2O_3 is obtained. The comparison of the widths of the XRD peaks of the crystalline Fe_3O_4 and those of commercial Fe_3O_4 shows that the former are much broader, implying that the particle size of crystalline Fe_3O_4 is smaller than that of commercial Fe_3O_4. The particle size calculated for the amorphous product from the line broadening of X-ray powder diffraction[22] was 12 nm.

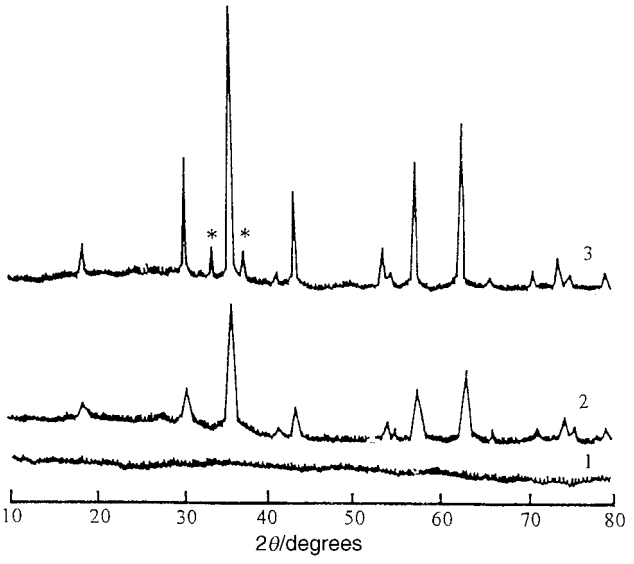

Fig. 1 XRD patterns of (1) amorphous Fe_2O_3, (2) crystalline Fe_3O_4, obtained after heating amorphous Fe_2O_3 at 425 °C for 1 h under nitrogen and (3) commercial Fe_3O_4. The asterisked peaks should not appear if Fe_3O_4 is of high purity.

Fig. 2 shows TEM images of amorphous Fe_2O_3 powders. There is no evidence for crystallite formation of Fe_2O_3 powder obtained from the sonication of $Fe(CO)_5$ under air. The amorphous Fe_2O_3 powder is an agglomerate of small particles. Most of the particles are aggregated in a spongelike form, and therefore, it is very difficult to accurately determine the individual particle sizes. Products obtained from the sonication of pure $Fe(CO)_5$ and 4, 1 and 0.25 M solutions of $Fe(CO)_5$ in decalin are denoted A, B, C and D, respectively. From these TEM images, we observe a gradual change from product A to D, *i.e.* with decrease of $Fe(CO)_5$ concentration in decalin the product becomes less agglomerated and more porous.

A direct way to determine particle size is the application of submicrometre particle size analysis. Although most of the particles of the amorphous samples are highly agglomerated, we can still measure the mean size of these particles. A measured amount of amorphous Fe_2O_3 powder (*ca.* 2 mg) was mixed with ethylene glycol (10 ml) and the mixture was sonicated in an ultrasonic bath for 30 min to form a colloid. This colloid was analysed immediately. The mean particle sizes were 233 nm (A), 187 nm (B), 147 nm (C) and 142 nm (D). This result strongly suggests that during sonication the amorphous Fe_2O_3 particles in solution have less opportunity to be agglomerated, and therefore the product is more porous and more spongelike as shown in the TEM pictures.

DSC and TG

Fig. 3 shows DSC traces for all the four samples. The endothermic peak at *ca.* 150 °C is attributed to the desorption of

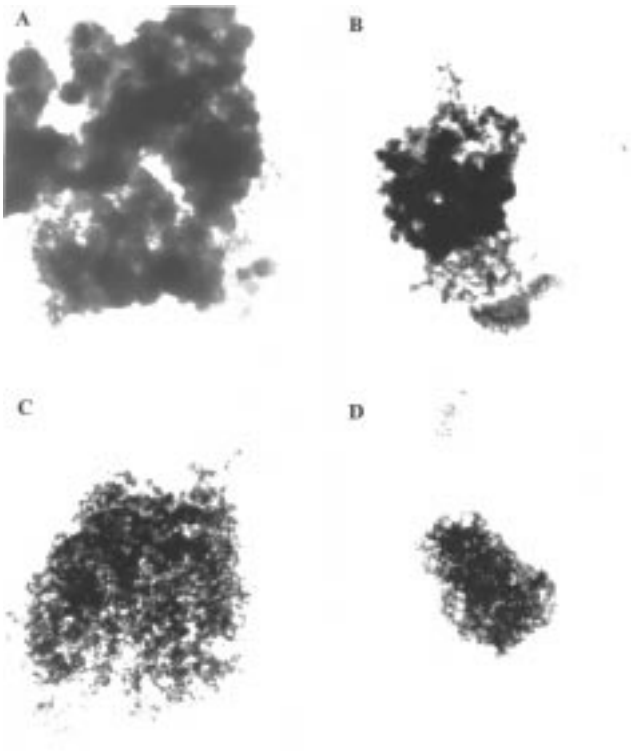

Fig. 2 TEM pictures of amorphous Fe_2O_3. A, B, C and D correspond to the products of the irradiation of pure $Fe(CO)_5$ and its 4.0, 1.0 and 0.25 M solutions in decalin, respectively.

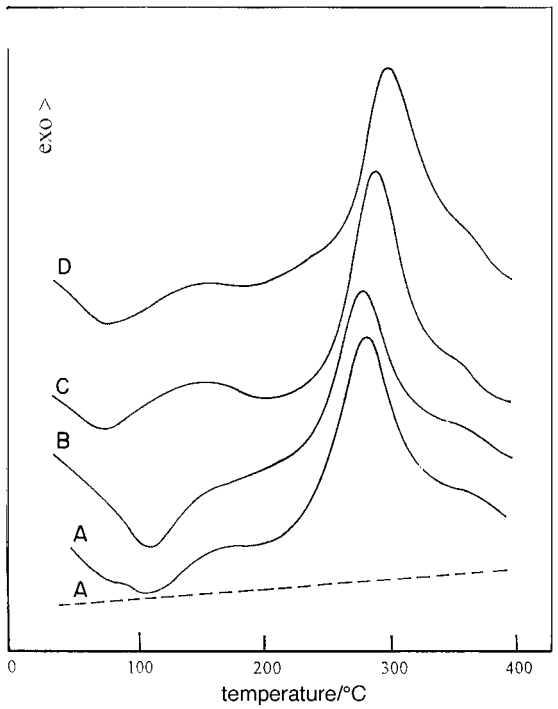

Fig. 3 DSC curves of amorphous Fe_2O_3 before heat treatment (solid line) and after heating to 400 °C (dashed line). Heating rate: 10 K min^{-1}, N_2 (99.999%) is used in these experiments. A, B, C and D correspond to the products of the irradiation of pure $Fe(CO)_5$ and 4.0, 1.0 and 0.25 M solutions in decalin, respectively.

contaminants [such as $Fe(CO)_5$] from the surface of the product. The large exothermic transition is assigned as corresponding to the crystallization of amorphous Fe_2O_3. The crystallization temperature increases from 280 °C for A to 298 °C for D. The TEM results indicate that particles of A are denser than those of the other samples and therefore it may be easier for these dense particles to be crystallized resulting in a lower crystallization temperature. The heat of transition from the amorphous to the crystalline state is *ca.* 38 ± 4 kJ mol^{-1}, no distinct differences were found between the four samples.

Fig. 4 shows the TG trace for amorphous Fe_2O_3 powder.

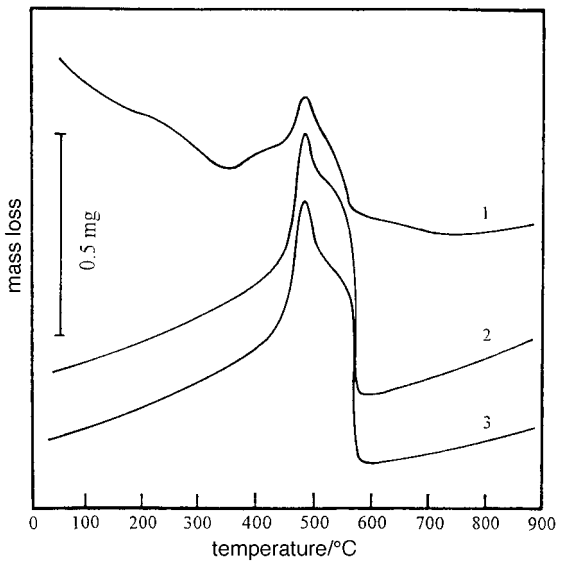

Fig. 4 Magnetic TG curves of amorphous Fe_2O_3 [prepared from pure $Fe(CO)_5$]: (1) before heat treatment; (2) after heating to 900 °C under nitrogen (conversion to Fe_3O_4) and (3) commercial Fe_3O_4. Heating rate: 10 K min^{-1}, N_2 (99.999%) is used in these experiments.

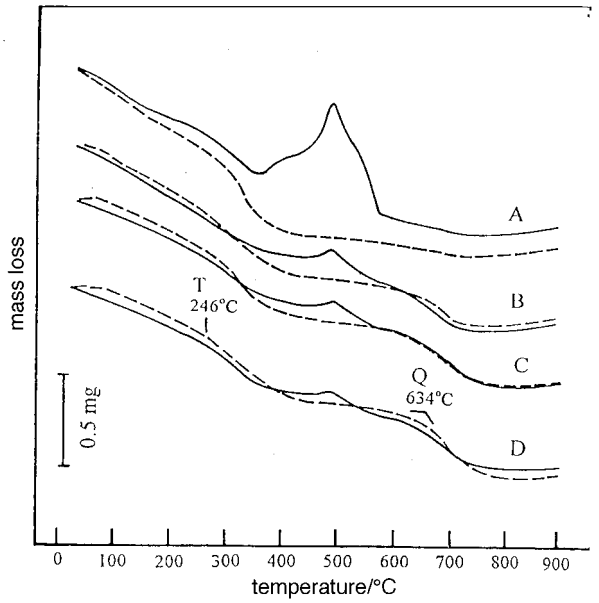

Fig. 5 TG curves of amorphous Fe_2O_3 with (solid line) and without (dashed line) an external permanent magnet. Heating rate: 10 K min^{-1}, N_2 (99.999%) is flowed through the system. A, B, C and D correspond to the products of the irradiation of pure $Fe(CO)_5$ and its 4.0, 1.0 and 0.25 M solutions in decalin, respectively. T and Q are the temperatures for the turning points in the mass losses (see text).

After heating to 900 °C under nitrogen (leading to crystallization), the sample loses its amorphous character and has the same magnetic behavior as that of commercial γ-Fe_3O_4, further proving that the product from the sonication, amorphous Fe_2O_3, is converted into crystalline Fe_3O_4 when heated in nitrogen. The sharp drop in mass detected around 570 °C is attributed to the Curie point of Fe_3O_4.[15] In the TG curve in the absence of a magnetic field (Fig. 5) it is seen that amorphous Fe_2O_3 loses mass in two steps: one above 300 °C and the other above 630 °C. We attribute the mass loss at about 300 °C to the conversion of Fe_2O_3 to Fe_3O_4 which is accompanied by a loss of 0.5 moles of oxygen. The mass loss at above 630 °C (point Q) is associated with evaporation of nanocrystals of Fe_3O_4 powder in the gas flow of the TG oven. This is a speculative interpretation, however: at this temperature all the organic impurities have long since been desorbed. We explain this relatively low temperature of vaporization as a consequence of the small particle size. The decomposition and the loss of oxygen is also dependent on particle size. The smaller the particles or the more porous the sample, the easier is its decomposition. The mass loss temperature decreases from 304 °C for product A to 246 °C (point T) for product D. Fig. 5 which shows TG traces measured in the presence of a permanent magnetic field shows also that the magnetization decreases from the product A to product D. No Curie point can be observed in the TG curve of amorphous Fe_2O_3.

Magnetization measurements

The magnetization of ferromagnetic materials is very sensitive to the microstructure of a particular sample. If a specimen consists of small particles, its total magnetization decreases with the particle size owing to an increase in the dispersion of the exchange integral[23] which finally reaches the superparamagnetic state, when each particle acts as a big 'spin' with suppressed exchange interaction between the particles. For a theoretical description of the magnetic behavior of materials consisting of interacting nanoparticles the reader is referred to ref. 24. Thus, we expect to see a dramatic difference between the magnetization of a commercial Fe_2O_3 powder and that of the amorphous sample and Fig. 6 clearly demonstrates this

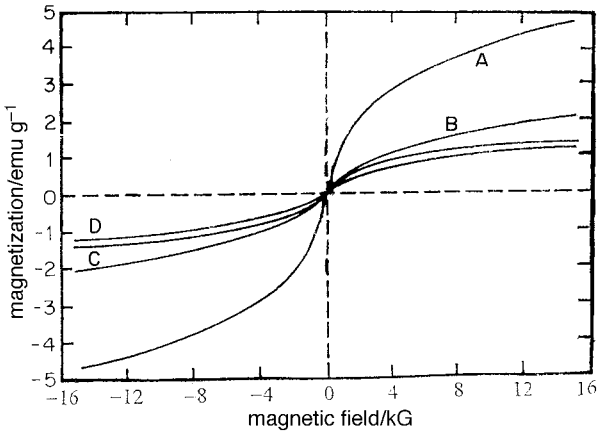

Fig. 6 Magnetization curves of amorphous Fe_2O_3 at room temperature. A, B, C and D correspond to the products of the irradiation of pure $Fe(CO)_5$ and its 4.0, 1.0 and 0.25 M solutions in decalin, respectively.

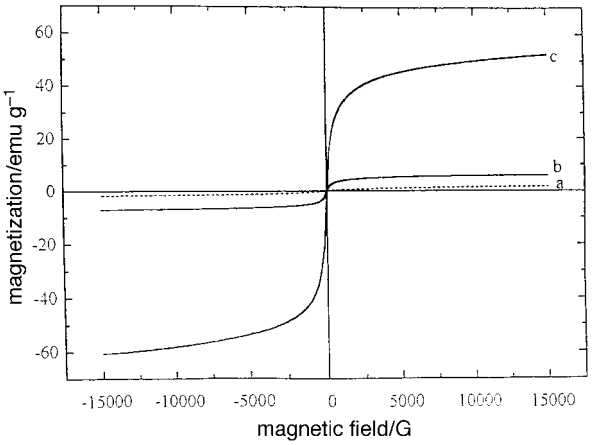

Fig. 7 Magnetization curves of: (a) as-prepared amorphous Fe_2O_3; (b) α-Fe_2O_3 prepared by heating amorphous Fe_2O_3 for 24 h at 430 °C under oxygen and (c) γ-Fe_2O_3 obtained by heating amorphous Fe_2O_3 for 3 h at 370 °C under oxygen

effect. The coercivity field H_c and magnetization M at the external magnetic field of 1.5 T of amorphous Fe_2O_3 are 25 G and 1.44 emu g^{-1}, (product C), whereas for commercial γ-Fe_2O_3 we find $H_c = 293$ G and $M(H = 1.5\ T) = 96$ emu g^{-1}. It is important to note, that we observe no saturation of magnetization as a function of the field and no hysteresis for the amorphous Fe_2O_3, which is further evidence that we are dealing with a superparamagnetic material. Moreover, we stress that at room temperature and magnetic field sweep rate of 35 G s^{-1}, our sample is still above the blocking temperature, indicating that the compound is not in the spin-glass regime. Finally, we conclude that the magnetization measurements confirm that our sample consists of nanoparticles small enough to exhibit superparamagnetic behavior.

Fig. 6 demonstrates also the gradual change in the magnetization as a function of the concentration of the initial $Fe(CO)_5$ solution and is related to the dependence of the magnetization on the particle size. At 15 kG, the magnetization of commercial γ-Fe_2O_3 saturates at a value of 96 emu g^{-1}. By contrast, our amorphous samples do not exhibit saturation and their magnetization values are much lower than that of commercial Fe_2O_3. The magnetization (at 15 kG) decreases gradually from 4.72 emu g^{-1} for product A to 1.30 emu g^{-1} the product D. We explain these results as follows. In bulk ferromagnetic materials, the local magnetic moments are organized in domains with a certain characteristic size. This yields a reduction in magnetic energy of the demagnetizing field surrounding the sample. The total energy of domain boundaries is proportional to the square of the effective radius of a sample, whereas the magnetic energy of the demagnetizing field shows a cubic proportionality. At a given particle size the particles become single-domain (all spins oriented in a certain direction). In this case, the material becomes superparamagnetic and does not exhibit saturation. From Fig. 6 we can see that amorphous Fe_2O_3 is superparamagnetic and the magnetization decreases from product A to D, indicating that the particle size decreases from A to D. Fig. 7 compares the room-temperature magnetization loops of amorphous Fe_2O_3 with that of crystalline α-Fe_2O_3 and γ-Fe_2O_3 prepared by heating the amorphous iron oxide according to the above-mentioned procedures. The former, α-Fe_2O_3, is known as weakly ferromagnetic while the later is ferrimagnetic at room temperature. According to the above-mentioned measurements, the saturation magnetization of commercial γ-Fe_2O_3 is 96 emu g^{-1}. In Fig. 7 the γ-Fe_2O_3 curve does not saturate and reaches a value of 53 emu g^{-1} at 15 kG. This indicates that despite the agglomeration and sintering that take place upon heating (see next section) the particle size is still small.

Table 1 summarizes the TG, DSC and magnetization results as a function of the concentration of the $Fe(CO)_5$ solution.

Surface area measurements

To further substantiate our claim for the particle size dependence, surface area measurements were carried out based on the BET method. The results presented in Table 2 show the increase in the surface area of the amorphous Fe_2O_3 from A to D. This increase is also seen for crystalline γ-Fe_2O_3 obtained from A to D. Comparison between amorphous and crystalline Fe_2O_3 shows a drastic reduction of surface area upon crystallization. This is accounted for by agglomeration and sintering of the metal oxide clusters that occurs upon heating of the amorphous material. Similar results were obtained in our study

Table 2 Surface area (S) of Fe_2O_3 as a function of the concentration of the sonicated $Fe(CO)_5$ in decalin solution

[$Fe(CO)_5$]/M	$S_{amorphous}$/m^2 g^{-1}	$S_{crystalline}$/m^2 g^{-1}
0.25	207	82
1.00	181	67
4.00	148	46
—[a]	79	10

[a]Neat $Fe(CO)_5$.

Table 1 TG, DSC and magnetization results for amorphous Fe_2O_3

			TG[b]		
sample	mean size/A°	DSC cryst. temp./°C[a]	T/°C	Q/°C	magnetization/emu g^{-1}
A	233	280	304	637	4.72
B	187	277	265	630	2.17
C	147	290	265	636	1.35
D	142	298	246	634	1.30

[a]cryst. temp. = crystallization temperature. [b]In absence of an applied magnetic field.

of the deposition of nanophasic amorphous nickel on silica microspheres.[19] The crystallization of the amorphous nickel reduced the surface area from 28 to 12 $m^2\ g^{-1}$.

Conclusions

In this work, we have studied the synthesis of amorphous Fe_2O_3 with different particle sizes, and the influence of the particle size on the magnetic behavior of amorphous Fe_2O_3. Amorphous Fe_2O_3 can be obtained by the sonication of $Fe(CO)_5$ in air and our experimental results show that the particle size can be controlled by the concentration of $Fe(CO)_5$ in decalin during sonication. The lower the concentration of $Fe(CO)_5$, the smaller the particle size of the amorphous Fe_2O_3. DSC shows that amorphous Fe_2O_3 with smaller particle size has a higher crystallization temperature. Magnetization measurements establish that amorphous Fe_2O_3 has superparamagnetic character and the magnetization is reduced gradually from 4.72 emu g^{-1} for product A to 1.30 emu g^{-1} for product D.

Dr. Yu. Koltypin thanks the Ministry of Absorption, the Center for Absorption in Sciences, for their financial help. Prof. A. Gedanken is grateful to Bar-Ilan Research Authorities for supporting this project. This research was also supported by grant 94-00230 from the US–Israel Binational Science Foundation (BSF), Jerusalem, Israel. We thank Prof. Y. Yeshurun for helpful discussions and for making available for this study the facilities of the National Center for Magnetic Measurements at the Department of Physics, Bar-Ilan University. The study of the magnetic properties is supported by the Israel Science Foundation administered by the Israeli Academy of Science and Humanities. The authors wish to thank Prof. M. Deutsch, Department of Physics, Bar-Ilan University, for extending the XRD facility to us.

References

1 J. Livage, *J. Phys*., 1981, **42**, 981.
2 *Ferromagnetic Materials*, ed. E. P. Wohlfarth, North-Holland, Amsterdam–New York–Oxford–Tokyo, 1980, vol. 2, p. 405.
3 L. Murawski, C. H. Chung and J. D. Mackenzie, *J. Non-Cryst. Solids*, 1979, **32**, 91.
4 H. Edward Curry-Hyde, H. Musch and A. Baiker, *Appl. Catal*., 1990, **65**, 211.
5 H. Cao and S. L. Suib, *J. Am. Chem. Soc*., 1994, **116**, 5334.
6 M. Sugimoto, *J. Magn. Magn. Mater*., 1994**, 133**, 460.
7 K. Tanaka, K. Hirao and N. Soga, *J. Appl. Phys*., 1991, **69**, 7752.
8 M. Sugimoto and N. Hiratsuka, *J. Magn. Magn. Mater*., 1983, **31/34**, 1533.
9 W. E. Steger, H. Landmesser, U. Boettcher and E. J. Schubert, *Mol. Struc*., 1990, **217**, 341.
10 B. Pashmakov, B. Claflin and H. Fritzsche, *Solid State Commun*., 1993, **86**, 619.
11 K. Kandori and T. Ishikawa, *Langmuir*, 1991, **7**, 2213.
12 K. S. Suslick, S. B. Choe, A. A. Cichowlas and M. W. Grinstaff, *Nature* (*London*), 1991, **353**, 414.
13 K. S. Suslick, M. Fang, T. Hyeon, T. and A. A. Cichowlas, *Molecularly Designed Ultrafine Nanostructured Materials*, ed. K. E. Gonsalves and G. M. Chow, Pittsburgh, PA, 1994, pp. 443–448.
14 K. S. Suslick, T. Hyeon, M. Fang and A. A. Cichowlas, *Molecularly Designed Ultrafine Nanostructured Materials*, ed. K. E. Gonsalves and G. M. Chow, Pittsburgh, PA, 1994, pp. 201–206.
15 M. W. Grinstaff, M. B. Salamon and K. S. Suslick, *Phys. Res. Rev. B*, 1993, **48**, 269.
16 X. Cao, Yu. Koltypin, G. Kataby, R. Prozorov and A. Gedanken, *J. Mater. Res*., 1995, **10**, 2952.
17 X. Cao, Yu. Koltypin, G. Kataby, R. Prozorov and A. Gedanken, *J. Mater. Res*., 1997**, 12**, 402.
18 Yu. Koltypin, X. Cao, G. Kataby, R. Prozorov and A. Gedanken, *J. Non-Cryst. Solids*, 1996, **201**, 159.
19 S. Ramesh, Yu. Koltypin, R. Prozorov and A. Gedanken, *Chem. Mater*., 1997, **9**, 546.
20 F. Feigel, *Spot Tests, Inorganic Applications*, Elsevier, New York, 1954, vol. 1, pp. 154–155.
21 F. A. Cotton and G. Wilkinson, *Advanced Inorganic Chemistry*, Wiley Interscience, New York, 1962, p. 709.
22 D. Segal, *Chemical Synthesis of Advanced Ceramic Materials*, Cambridge University Press, New York, 1989, p. 150.
23 S. R. Elliott, *Physics of Amorphous Materials*, Longman, London and New York, 1984, pp. 350–3457.
24 S. Morup, *Europhys. Lett*., 1994, **28**, 671; S. Morup and E. Tronc, *Phys. Rev. Lett*., 1994, **72**, 3278.

Paper 7/04003B; *Received* 10*th June*, 1997